

Metamaterial tuning by manipulation of near-field interaction

David A. Powell,^{1,*} Mikhail Lapine,^{2,1} Maxim Gorkunov,³ Ilya V. Shadrivov,¹ and Yuri S. Kivshar¹

¹*Nonlinear Physics Centre, Research School of Physics and Engineering,
Australian National University, Canberra ACT 0200, Australia*

²*Dept. Electronics and Electromagnetics, Faculty of Physics,
University of Seville, Avda. Reina Mercedes s/n, 41015 Seville, Spain*

³*A. V. Shubnikov Institute of Crystallography, Russian Academy of Sciences, Leninski prosp. 59, 119333 Moscow, Russia*

We analyze the near-field interaction between the resonant sub-wavelength elements of a metamaterial. We show that by adjusting the lattice configuration it becomes possible to manipulate this near-field interaction, and thus tune the magnetic response of a lattice of split-ring resonators. By studying the case of a pair of split-ring resonators, we are able to show the coupling mechanisms at work and how they influence the response of the complete metamaterial structure. We use the results of this analysis to explain experimentally observed tuning of microwave metamaterial arrays.

I. INTRODUCTION

Metamaterials, which are typically regular arrays of sub-wavelength resonant particles, offer us a new degree of freedom in controlling the electromagnetic response of matter. Thus we are no longer completely constrained by the properties of existing materials, but can tailor the response in an almost arbitrary fashion, for example achieving very high¹, very low^{2,3}, and negative^{4,5} values of refractive index, permittivity and/or permeability. Because of the inherently strong dispersion of resonant metamaterials, they must be modified in order to operate in a different frequency band. Therefore there is a significant push to have a further degree of control over these materials — tunability of their response.

Fortunately, the engineered nature of metamaterials allows their properties to be controlled externally, either by dynamically modifying their structure, or by adding some nonlinear inclusion and controlling with external fields⁶. Examples of the latter approach include the introduction of varactor diodes^{7,8}, ferroelectrics⁹ and photo-conductive semi-conductors^{10,11}. On the other hand, even without resorting to such exotic (and often lossy) constituents, there is a great deal of freedom to manipulate the structure itself, and this is the approach we propose here. We consider specifically the split ring resonator (SRR) as one of the most important metamaterial elements, noting that whilst the fine details of near-field interaction are structurally specific, the concept of manipulating the lattice is very general and can be applied to a wide variety of structures.

An analytical model for the magnetic response of a sub-wavelength array of identically oriented wire loops loaded with a capacitance¹² takes into account the mutual interaction of all the elements in the lattice, which is essential for deriving the effective permeability correctly. Although that analysis is limited to the quasi-static case and accounts only for magnetic near-field interactions, it is crucial for revealing the consequence of lattice changes. These tend to be overlooked by more recent approaches which include spatial dispersion but are based on nearest-neighbor interaction¹³ or point-dipole approximation¹⁴.

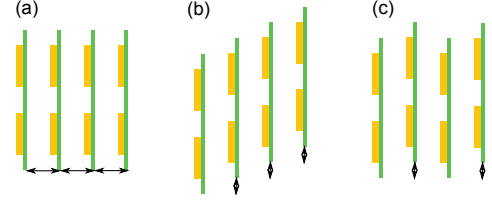


FIG. 1: (Color online) Several approaches to modify the lattice for metamaterial tunability: (a) changing lattice constant¹⁵, (b) continuously shifting layers¹⁶; and (c) superlattice of alternating shifts of layers¹⁶.

In particular, it has been pointed out¹² that the resonant frequency of the metamaterial permeability can be altered by varying the lattice constants without changing the structural units. This scheme is illustrated in Fig. 1(a), and has been verified by experiments in Ref. 15. However, a practical consequence of this change in lattice constant is that the sample size also changes correspondingly. More recently, an alternative approach was suggested in Ref. 16: introducing a shift between layers in order to create a monoclinic lattice, with the shift increasing linearly between layers, as shown in Fig. 1(b). This configuration keeps the density of elements within the metamaterial constant, and can tune the coupling between neighboring particles to modify the response of the complete metamaterial. However, for finite size samples, this shift inevitably results in a significant change in sample shapes. Thus, for practical purposes, we have proposed a superlattice type of geometry, whereby only every second layer is shifted by the same amount, as shown in Fig. 1(c). This tuning scheme proved to be robust, and allows significant manipulation of the resonant frequency with only a small change in the sample geometry¹⁶. Therefore the sample geometry and its effective properties can be engineered almost independently to achieve the desired manipulation of electromagnetic waves.

It turns out, however, that this structural tuning of metamaterials depends very strongly on the nature of the near field interactions. Since metamaterial elements such

as split ring resonators are not necessarily highly symmetric, *the relative orientation of particles within the lattice is of key importance*. In order to understand the coupling mechanisms and how they are affected by the lattice shift, it is useful to start with the simplest geometry — a pair of split rings. Several authors have conducted numerical and experimental investigations of coupling for different cases and effects, including the influence of gap orientation on the coupling between two rings in plane¹⁷, as well as the form of the polarizability tensor and the frequencies of higher order resonances for different ring geometries¹⁸. A detailed study was performed on how modifying the geometric arrangement of a pair of coupled 1D SRR arrays supporting magneto-inductive waves can be used to tailor the coupling between elements, and thus to engineer the dispersion curves¹⁹. Some particular cases of SRR radiative coupling were also presented²⁰.

Related effects were also analyzed in the optical domain in recent reports on the influence of rotation²¹ or distance²² on coupling between SRRs on the same axis, and in the attempts to overlap the frequencies of electric and magnetic resonances to achieve negative refractive index²³. Similar phenomena have also been considered in other metamaterial geometries, including coupling between several layers of weakly and strongly coupled fishnets²⁴ and coupling within in-plane superlattices^{25,26}.

In this paper, we present an in-depth analysis of the effect of the SRR offset introduced to create the superlattice shift. We show how it can be used as an additional degree of freedom to tune the metamaterial response. First, in Section II we give an overview of the basic theory behind metamaterial coupling, including a discussion of the limitations of analytical modeling of SRR arrays. Section III is devoted to the study of interaction between a pair of split-ring resonators subject to a lateral shift, and it explains quantitatively how the shift affects the position of the magnetic resonance. In Section IV we conduct a similar analysis of a bulk metamaterial and identify the mechanisms at work in the experimental tuning of a metamaterial slab in a waveguide. Finally, Section V concludes the paper with further discussions and outlook.

II. MAGNETIC INTERACTION IN METAMATERIALS

When inductive coupling is the dominant interaction mechanism between the SRRs in a metamaterial, we are able to consider an array of split rings as an array of current loops with some mutual inductance between them. One may use this model as a good starting point for understanding the mechanisms of the near-field interaction in metamaterials. It is fully within the framework of the effective permeability approach formulated in Ref. 12.

A further simplification often made in the literature is to assume that the metamaterial is equivalent to a lattice

of interacting point dipoles. However, such an approach requires the size of the elements to be much smaller than the smallest lattice constant. In most SRR metamaterials this is not the case, as the strong coupling between close neighboring elements is used to increase the bandwidth. The tuning by lattice manipulation also demands small distances between the elements.

According to Ref. 12, the effective permeability of the metamaterial can be rigorously calculated as:

$$\mu(\omega) = 1 - \frac{A\omega^2}{\omega^2 - \omega_r^2 + i\Gamma\omega} \quad (1)$$

with the resonant frequency

$$\omega_r = \omega_o \left(\frac{L_\Sigma}{L} + \frac{\mu_o \nu S^2}{3L} \right)^{-1/2}. \quad (2)$$

One can see that the resonance of metamaterial is not only determined by the SRR density ν and properties of individual elements, such as the resonant frequency of a single element ω_o , its self-inductance L and effective geometric cross-section S . A major role is also played by the mutual interaction of elements in the lattice, which can be accounted for by the effective mutual inductance

$$L_\Sigma = L + \sum_{n' \neq n} L_{nn'} \quad (3)$$

where the sum runs over all the elements in a physically small volume where the average macroscopic field is evaluated. In particular, for thin wire loops, the mutual inductance terms $L_{nn'}$ can be found²⁷ from a simple numerical integration (for this approach, excluding retardation):

$$L_{nn'}(\bar{r}) = \frac{\mu_0 r_0^2}{4\pi} \int_0^{2\pi} \int_0^{2\pi} d\varphi_1 d\varphi_2 \cos(\varphi_1 - \varphi_2) \times \\ [\rho^2 + z^2 + 2r_0^2(1 - \cos(\varphi_1 - \varphi_2)) + 2\rho r_0(\cos \varphi_2 - \cos \varphi_1)]^{-\frac{1}{2}},$$

where the distance vector \mathbf{r} between the ring centers has been decomposed into a radial component ρ and axial component z , r_0 is the ring radius and φ_1 and φ_2 represent the angular variables running along each ring. Asymptotically this interaction decays as $1/r$, so while the nearest neighbors provide the strongest contribution, they do not necessarily dominate over all others. Clearly, this interaction is highly anisotropic¹⁹, the mutual inductance being positive for the rings on the same axis, but negative for the rings in the same plane.

Importantly, this approach does not account for capacitive interaction between the rings, which may also affect the resonant properties considerably, depending on the geometry of resonators²⁸. For a pair of coaxial rings, the total interaction can be reliably modeled as a circular parallel conductor transmission line, as for broadside-coupled split-ring resonators²⁹ or, alternatively, with an

extended circuit model accounting for the distributed capacitance and inductance³⁰. However, for the case of mutually shifted rings, these approaches no longer apply and a quantitative analysis can be done by studying the interaction of modes excited in the SRRs. Below we show the main features of such an approach in the simple case of a pair of SRRs.

III. INTERACTION BETWEEN A PAIR OF SPLIT-RINGS RESONATORS

In order to understand the essential features of the near-field interactions in metamaterials, it is useful to study the canonical case of coupling of a pair of elements. In this Section we focus on a pair of SRRs, either identically (gap-to-gap) oriented or rotated by 180° with respect to each other (as in the broadside-coupled SRR), and subject to a lateral offset δa (see the geometry and incident polarization shown in Fig. 2).

Considering a single SRR, it is known that it possesses a discrete set of eigenmodes (standing waves) with corresponding eigenfrequencies. In an arbitrarily excited SRR, the currents and charges can be represented as a superposition of the eigenmodes. The fundamental mode with the lowest frequency is relevant for the magnetic resonance in SRRs. On the frequency scale this mode is well isolated from the higher-order modes, and we can restrict ourselves to the single-mode approximation neglecting the excitation of higher modes.

The time dependent charge density ρ and current density \mathbf{J} in a resonant element with excited fundamental mode can be written in the most general form of a standing wave:

$$\rho(\mathbf{x}, t) = Q(t)q(\mathbf{x}), \quad (4)$$

$$\mathbf{J}(\mathbf{x}, t) = I(t)\mathbf{j}(\mathbf{x}), \quad (5)$$

where q and \mathbf{J} describe the charge and current distribution in space. In SRRs, the variation of the current distribution across the width of the conductive track could be neglected, however for generality our approach takes into account the complete 3-dimensional surface-current distribution.

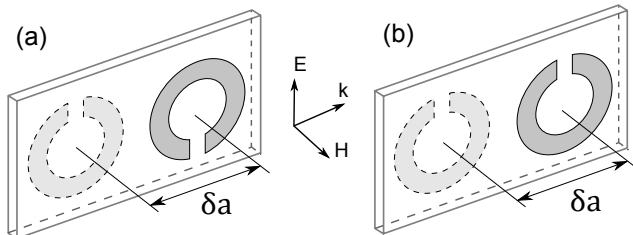


FIG. 2: (Color online) Geometry of the pair of rings (a) broadside-coupled and (b) gap-to-gap orientation

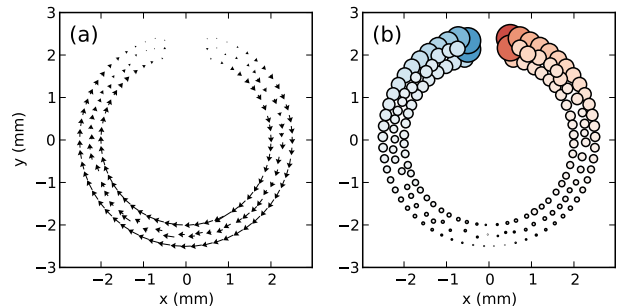


FIG. 3: Numerically calculated (a) current and (b) charge distribution across an SRR at resonance

To satisfy the conservation of charge

$$\nabla \cdot \mathbf{J} = -\frac{\partial \rho(\mathbf{x}, t)}{\partial t} \quad (6)$$

we imply that

$$I(t) = \dot{Q}(t), \quad (7)$$

$$\nabla \cdot \mathbf{j}(\mathbf{x}) = -q(\mathbf{x}). \quad (8)$$

Thus if the the current is known, it is easy to find the charge distribution and vice-versa. The mode profile obtained numerically for our SRR geometry is shown in Fig. 3. The current \mathbf{j} is symmetric and reaches its maximum at the point opposite to the gap. In accordance with Eq. (8), the charge distribution $q(\mathbf{x})$ is antisymmetric and goes through zero where $\mathbf{j}(\mathbf{x})$ is maximal. We see that $q(\mathbf{x})$ reaches its maximal and minimal values near the gap.

In the single mode approximation, the dynamics of the SRR can be fully described by the time-dependent amplitude $Q(t)$, and we may write the SRR Lagrangian as a sum of terms quadratic in Q and \dot{Q} :

$$\mathcal{L} = A\dot{Q}^2 - BQ^2, \quad (9)$$

where A and B are constants which will be discussed below. Note that a possible term $\dot{Q}Q$ is a full time derivative and can be skipped.

Accordingly, the SRR energy reads:

$$E = \dot{Q} \frac{\partial \mathcal{L}}{\partial \dot{Q}} - \mathcal{L} = AI^2 + BQ^2, \quad (10)$$

and is nicely separated into inductive (magnetic) and capacitive (electric) parts. Clearly, stability of the SRR requires $A \geq 0$, $B \geq 0$.

The Lagrangian equation of motion

$$\frac{d}{dt} \frac{\partial \mathcal{L}}{\partial \dot{Q}} = \frac{\partial \mathcal{L}}{\partial Q} \quad (11)$$

yields that the dynamics of a single SRR is described by the oscillator equation for the charge amplitude:

$$\ddot{Q}(t) + \omega_0^2 Q(t) = 0, \quad (12)$$

and the fundamental mode resonance occurs at the frequency $\omega_0 = \sqrt{B/A}$.

These results appear similar to the Lagrangian formalism based on an equivalent circuit model³¹. Indeed, one could identify $2A$ and $1/2B$ as the inductance and capacitance, respectively. However, here we derive them explicitly from the mode shape and note that they do not necessarily agree with parameters calculated from a low-frequency circuit analysis such as Section II. Additionally, to find the resonant frequency, we do not need to calculate A and B explicitly, only their ratio.

For a pair of SRRs, the Lagrangian can be written as a sum of the single SRR Lagrangians and coupling terms, which we also write as quadratic in currents and charges:

$$\mathcal{L} = A(\dot{Q}_1^2 + \dot{Q}_2^2 + 2\alpha\dot{Q}_1\dot{Q}_2) - B(Q_1^2 + Q_2^2 + 2\beta Q_1Q_2). \quad (13)$$

The parameters α and β are the dimensionless constants of magnetic and electric near-field interactions respectively.

The corresponding Lagrangian equations of motion yield the system of ODEs for the time-dependent amplitudes $Q_{1,2}$:

$$\ddot{Q}_1 + \omega_0^2 Q_1 = -\alpha\ddot{Q}_2 - \beta\omega_0^2 Q_2, \quad (14)$$

$$\ddot{Q}_2 + \omega_0^2 Q_2 = -\alpha\ddot{Q}_1 - \beta\omega_0^2 Q_1, \quad (15)$$

Solving these equations one finds that a pair of resonators exhibits two resonances: symmetric and antisymmetric. For the symmetric resonance, $Q_1 = Q_2$, which yields the resonant frequency

$$\omega_S = \omega_0 \sqrt{\frac{1+\beta}{1+\alpha}}, \quad (16)$$

while the antisymmetric mode with $Q_1 = -Q_2$ has the frequency

$$\omega_{AS} = \omega_0 \sqrt{\frac{1-\beta}{1-\alpha}}. \quad (17)$$

The described resonance splitting is well known in the theory of harmonic oscillators. Generally, bringing together two oscillators of the same resonant frequency introduces coupling between them, which results in splitting into two modes. Examples have been shown of SRR resonant frequency as a function of some coupling parameter, e.g. mutual orientation¹⁷ or twist angle²¹, and typically demonstrate a splitting or hybridization of modes.

As we see, the direction and strength of the resonance shift are determined by the coupling constants α and β . To evaluate them, we use the expression for the electromagnetic energy following from the Lagrangian (13):

$$E = A(I_1^2 + I_2^2 + 2\alpha I_1 I_2) + B(Q_1^2 + Q_2^2 + 2\beta Q_1 Q_2). \quad (18)$$

The first group of terms gives the magnetic energy and the second group describes the electric energy.

A possible semi-analytical route to calculate α and β is to approximate the electric and magnetic response of

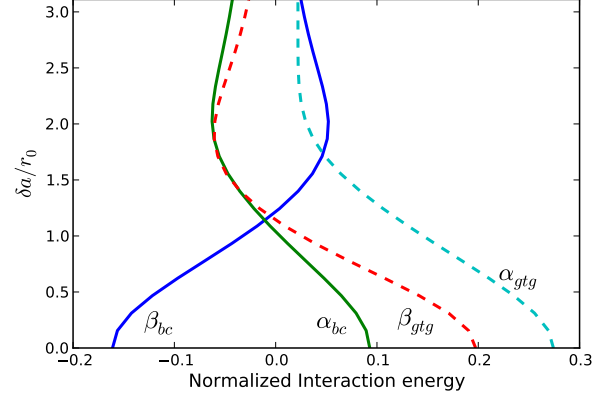


FIG. 4: Magnetic (α) and electric (β) coupling parameters for broadside coupled (bc) and gap-to-gap (gtg) orientation of a pair of SRRs.

each ring by a few terms of the multipole expansion. The problem with this approach is that it is based on the assumption that the observer (i.e. the second SRR) is at a large distance compared to the dimensions of the source. This requirement is strongly violated in our metamaterial samples, where the separation between rings is actually much smaller than the outer ring diameter.

Therefore we have chosen to calculate α and β numerically from the known charge and current distributions, $q(\mathbf{x})$ and $\mathbf{j}(\mathbf{x})$, of the fundamental mode in a single SRR. Indeed, in the single mode approximation, the energy of a pair of SRRs reads

$$E = Q_1^2 W_{E,11} + Q_2^2 W_{E,22} + 2Q_1 Q_2 W_{E,12} + I_1^2 W_{H,11} + I_2^2 W_{H,22} + 2I_1 I_2 W_{H,12}, \quad (19)$$

where the parameters:

$$W_{E,mn} = \int_{V_m} d^3x \int_{V_n} d^3x' \frac{q(\mathbf{x})q(\mathbf{x}')}{4\pi\epsilon_0|\mathbf{x}-\mathbf{x}'|}, \quad (20)$$

$$W_{H,mn} = \int_{V_m} d^3x \int_{V_n} d^3x' \frac{\mu_0 \mathbf{j}(\mathbf{x}) \cdot \mathbf{j}(\mathbf{x}')}{4\pi|\mathbf{x}-\mathbf{x}'|}. \quad (21)$$

The integrals can be easily evaluated once the charge and current distributions are known. The integrations over \mathbf{x} and \mathbf{x}' are over the same ring³³ if $m = n$ or over different rings otherwise. Accordingly, V_1 is a volume containing only the first ring, and V_2 is a volume containing only the second.

Comparing Eqs. (18) and (19) shows that the coupling parameters can be evaluated as

$$\alpha = \frac{W_{H,12}}{W_{H,11}}, \quad \beta = \frac{W_{E,12}}{W_{E,11}}. \quad (22)$$

We plot them for our chosen ring geometry in Fig. 4, for different offsets between the rings (normalized to the ring

radius). It can be seen that the electric coupling parameter β is nearly symmetric between the two configurations. This is due to the known symmetry of the fundamental mode, which approximately undergoes a sign inversion upon the up-down flip of the SRR. In the broadside-coupled configuration with no offset, the charges accumulated on the closest sides of the SRRs have opposite signs, $W_{E,12} < 0$, and β is also negative. Similarly, in the gap-to-gap orientation, the closest charges are of the same sign and the parameter $\beta > 0$.

At an offset of about one ring radius ($\delta a \approx r_0$), the charge on one ring is approximately equidistant from both positive and negative charges on the opposite ring, thus the net coupling passes through zero. At larger offsets, the electric coupling changes its sign but remains smaller, since only the nearest halves of the SRRs are effectively interacting, with this interaction decaying towards zero as the offset increases.

The magnetic interaction energy is also quite different for the two orientations. For the broadside-coupled case, the situation is similar to what we would expect from the simple analysis of wire loops with homogeneous current. At low offset, the magnetic field of one ring cuts through the other ring in the same direction to the surface normal, thus reinforcing the magnetic field and increasing the total energy. As the offset is increased, the situation gradually shifts to become like a pair of loops in the same plane, where the field from one ring cuts through the other in the opposite direction with respect to the surface normal. Hence, α_{bc} undergoes a change in sign.

For the gap-to-gap orientation the magnetic interaction is much stronger for low δa . This is due to the inhomogeneous current distribution, which is maximal opposite the gap. These maxima are located near each other and produce a stronger contribution to the integral in $W_{H,12}$ thus increasing α . As the rings are further separated from each other, the interaction energy reduces, but *does not undergo a change of sign*. We can intuitively understand this by neglecting the small contributions of the current in the region near the gaps, thus we effectively have two linear current elements in the same plane which always interact with the same sign. However, this balance is not universal and is determined by the specific geometry and parameters. To check this, we studied a geometry with smaller spacing between the rings, and another geometry with a very small gap, so that the current distribution was much more homogeneous, with lower resonance frequency. In both these cases (not shown) the magnetic coupling did change sign, and for the small gap the relative orientation had almost no impact, as expected in the quasi-static theory presented in Section II.

In order to verify that the calculated coupling correctly describes the frequency splitting of this system, we compare the frequency shift predicted by Eq. (16) and (17) with that obtained from the fully numeric wave simulations. We study SRRs with the same geometry as used in the experimental work (see below): mean

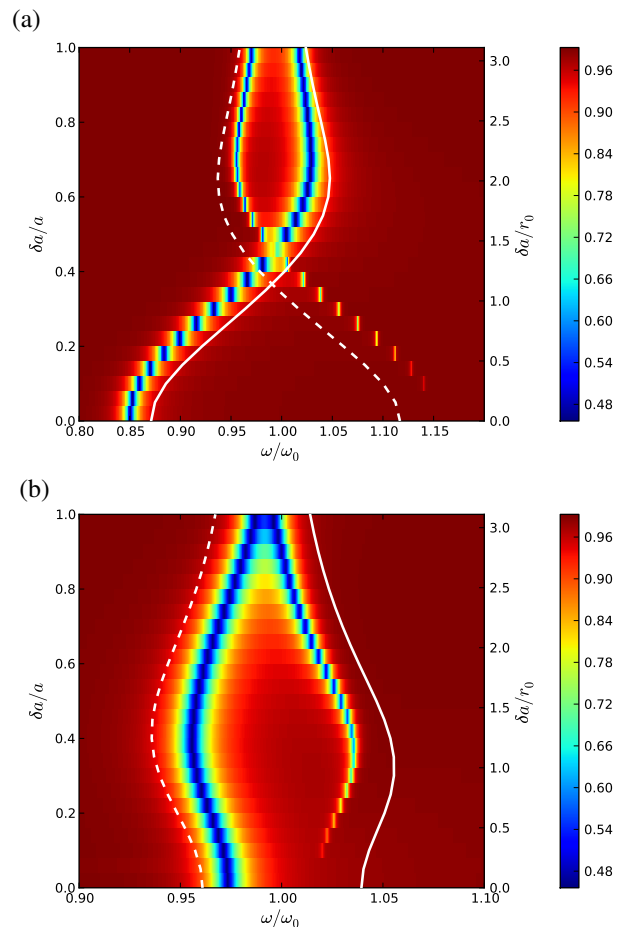


FIG. 5: (Color online) Numerical results. Transmission spectrum for a pair of (a) broadside-coupled and (b) gap-to-gap oriented rings. Solid line: ω_S from Eq. (16), broken line: ω_{AS} from Eq. (17)

radius $r_0 = 2.25\text{mm}$, track width 0.5mm and gap size 1mm , although for consistency with our interaction energy approach we assume a homogeneous background (in this case, free space). We use the frequency domain solver of the commercial software package CST Microwave Studio³² to model a pair of rings, in a unit cell with periodic boundary conditions in the directions transverse to the propagation direction. The periodic boundaries, however, are far enough from the two rings that they can be considered isolated.

The transmission spectrum as a function of offset is plotted in Fig. 5. We see that all the important features of the mode splitting are represented correctly by our single-mode theory of coupled SRRs, although the quantitative agreement is not exact. There are several reasons for this. Firstly, the minimum of transmission occurs at a frequency slightly different from the resonant frequency, due to impedance matching effects. Secondly, there may be some perturbation due to the coupling so that higher SRR eigenmodes may provide a minor contribution. Finally, our developed relations neglect retardation, which

is strictly valid in the sub-wavelength limit, whereas the the outer radius of the rings is 0.18λ at ω_0 .

We note also that the calculated transmission through the cell exhibits different depths of the resonance for the symmetric and antisymmetric modes. This is due to the different efficiency of coupling between the modes and the incident plane wave. For instance, it is impossible to excite the anti-symmetric mode for $\delta a = 0$, since the incident plane wave excites both rings in-phase.

IV. STRUCTURAL TUNABILITY OF METAMATERIALS

We now present experimental results for tuning the response of a slab of metamaterial. The metamaterial is fabricated using photolithography to etch copper tracks onto FR4 printed circuit board, using the same geometry as in our numerical simulation of a pair of rings. The fabricated sample has 30 layers, each with 5 rings in the propagation direction and is only one ring in height (i.e. a $5 \times 30 \times 1$ array). As with the pair of rings, we have assembled slabs with two relative orientations of the split rings in adjacent planes — gap-to-gap and broadside-coupled. In Fig. 6 we show the experimentally obtained transmission through each slab of closely coupled SRRs placed within WR229 rectangular metallic waveguide.

It can be seen that the orientation of the rings has a very drastic impact on the location of the resonance. For

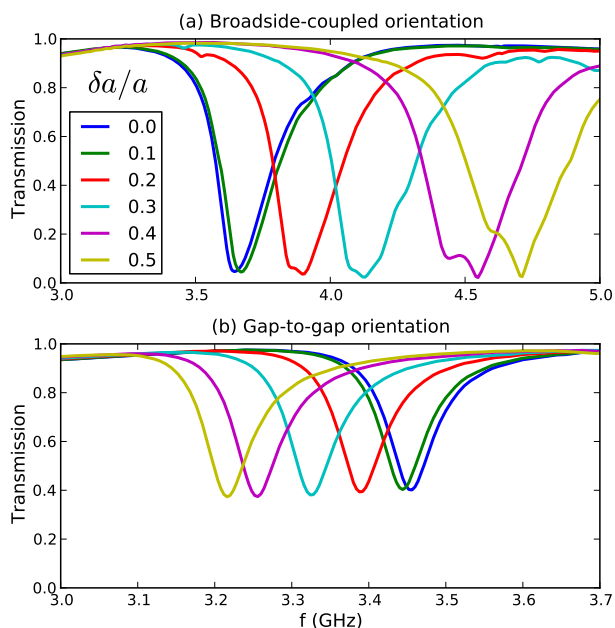


FIG. 6: (Color online) Experimental transmission while tuning $\delta a/a$ for split ring resonator slab in waveguide, for (a) broadside-coupled and (b) gap-to-gap orientation of adjacent layers. Note that the horizontal scale is different in the two plots.

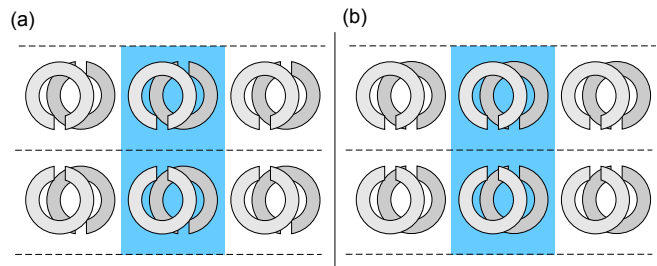


FIG. 7: Schematic of the effective super-lattice geometry corresponding to the waveguide measurement for (a) broadside-coupled and (b) gap-to-gap orientation. Dashed lines show planes of reflection symmetry, and the shaded region shows the super-cell with 4 SRRs.

the broadside-coupled orientation, the result is in good agreement with the results for a pair of rings presented in Section III, with very similar changes in the spectrum observed.

However, for the gap-to-gap orientation, the observed spectra are quite different. Moreover, numerical simulation of a system of two boards with 5 rings each, and *periodic boundaries* in both transverse directions (not shown), is qualitatively similar to the experimentally observed results but quantitatively highly inaccurate. The reason turns out to be the loss of symmetry when the system is placed inside the waveguide, because the upper and lower waveguide walls do not correspond to periodic boundaries, but instead represent planes of mirror reflection. Therefore, this system must be described as having a super-lattice arrangement in the vertical as well as horizontal planes, with each super-cell consisting of four SRRs. This cell has alternating orientation of the SRRs in the vertical direction corresponding to the planes of mirror symmetry, as shown in Fig. 7(b). Once this unit cell is taken into account, numerical simulations are in a good agreement with the experiment (Fig. 8(b)).

Naturally, numerical simulations for the broadside-coupled orientation also agree well with the experiment (Fig. 8(a)). In this case a very similar result is provided with simple periodic boundary conditions (not shown). For this orientation the super-lattice effectively formed by the waveguide shown in Fig. 7(a) does not have an essentially different symmetry to the original super-lattice.

We can conclude that in both cases the dominant mode of the slab corresponds to the dominant symmetric mode of a pair of rings, with a similar pattern of resonant frequency *vs.* offset occurring. We do not consider offsets greater than $0.5a$, since in an infinite lattice only shifts between 0 and 0.5 are unique, while in a finite structure, larger shifts result in very irregular boundaries. Note that in the simulations we have neglected the effect of the mode profile of the rectangular waveguide, which would correspond to an effective variation of the angle of incidence of the plane wave as a function of frequency, which can result in a different response due to the anisotropy and non-negligible spatial dispersion of the medium¹⁴.

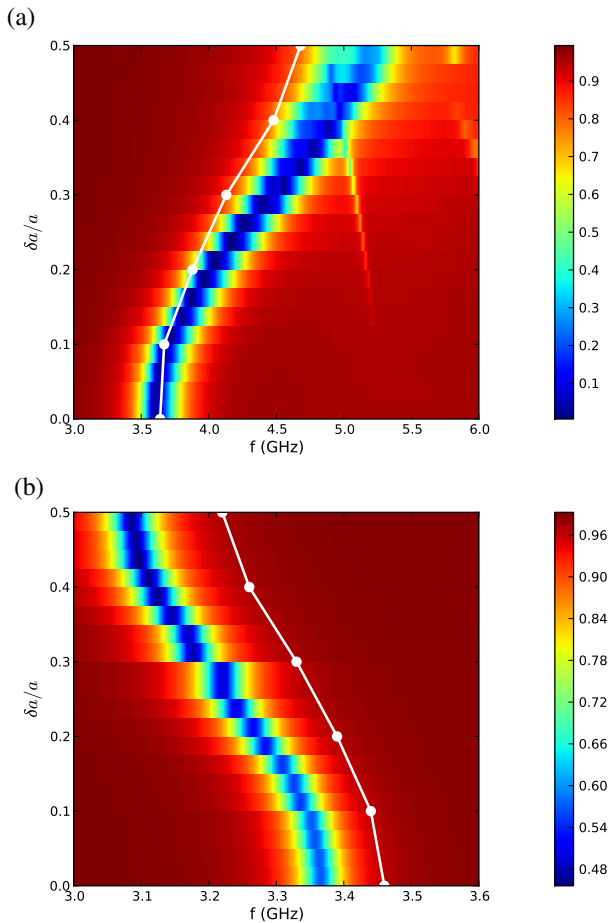


FIG. 8: (Color online) Numerically obtained transmission spectrum of metamaterial in waveguide, (a) broadside-coupled and (b) gap-to-gap orientation. The white line indicates experimentally obtained resonant frequencies.

Clearly the coupling in the complete lattice is much more complicated than in the simple two-ring system, as the interactions between a large number of rings must be taken into account. In principal it is possible to extend the analysis of Section III to an arbitrary number

of rings. However the qualitative agreement between the experimental results and the Lagrangian based formulation suggests that the phenomenology developed for the two rings is generally applicable and leads to correct predictions.

V. CONCLUSION

We have analyzed the near field coupling between split rings, considering both their relative orientation and the offset between their centers. Using a pair of rings as a model, we have shown the coupling mechanisms at work in our recently proposed tuning scheme, and confirmed that these mechanisms can predict qualitatively the performance of a realistic structure. This opens a road towards reliable design and development of tunable metamaterials for various applications.

We note that the specific geometry of the rings can have a very significant influence on the qualitative nature of the coupling, including cases which run counter to our intuitive understanding of current loops interacting magnetically. This is particularly important for metamaterials scaled down to operate at optical frequencies, where the paradigm of ideally conducting metal fails, while a consideration in terms of excitation and interaction of plasmonic standing waves provides a clear physical picture.

Acknowledgments

The authors are grateful to Dr. Lukas Jelinek and Prof. Ricardo Marqués (University of Seville) for helpful discussions. This work was supported by the Australian Research Council. M.L. acknowledges hospitality of Nonlinear Physics Centre and support of the Spanish Junta de Andalusia Project P06-TIC-01368. M.G. acknowledges support from the Russian Academy of Sciences, BPS Program “Physics of new materials and structures”.

* Electronic address: david.a.powell@anu.edu.au

¹ M. G. Silveirinha and C. A. Fernandes, Phys. Rev. B **78**, 033108 (2008).

² R. W. Ziolkowski, Phys. Rev. E **70**, 046608 (2004).

³ M. Silveirinha and N. Engheta, Phys. Rev. Lett. **97**, 157403 (2006).

⁴ J. Pendry, A. Holden, D. Robbins, and W. Stewart, IEEE Trans. Microwave Theory Tech. **47**, 2075 (1999).

⁵ D. R. Smith, W. J. Padilla, D. C. Vier, S. C. Nemat-Nasser, and S. Schultz, Phys. Rev. Lett. **84**, 4184 (2000).

⁶ M. Gorkunov and M. Lapine, Phys. Rev. B **70**, 235109 (2004).

⁷ O. Reynet and O. Acher, Appl. Phys. Lett. **84**, 1198

(2004).

⁸ I. Shadrivov, S. Morrison, and Y. Kivshar, Opt. Express **14**, 9344 (2006).

⁹ T. H. Hand and S. A. Cummer, J. Appl. Phys. **103**, 066105 (2008).

¹⁰ A. Degiron, J. Mock, and D. Smith, Opt. Express **15**, 1115 (2007).

¹¹ N.-H. Shen, M. Kafesaki, T. Koschny, L. Zhang, E. N. Economou, and C. M. Soukoulis, Physical Review B **79**, 161102 (2009).

¹² M. Gorkunov, M. Lapine, E. Shamonina, and K. Ringhofer, Eur. Phys. J. B **28**, 263 (2002).

¹³ J. Baena, L. Jelinek, R. Marqués, and M. Silveirinha, Phys.

- Rev. A **78**, 013842 (2008).
- ¹⁴ C. R. Simovski, *Metamaterials* **2**, 169 (2008).
 - ¹⁵ I. V. Shadrivov, D. A. Powell, S. K. Morrison, Y. S. Kivshar, and G. N. Milford, *Appl. Phys. Lett.* **90**, 201919 (2007).
 - ¹⁶ M. Lapine, D. Powell, M. Gorkunov, I. Shadrivov, R. Marques, and Y. Kivshar, *Appl. Phys. Lett.* **95**, 084105 (2009).
 - ¹⁷ F. Hesmer, E. Tatartschuk, O. Zhuromskyy, A. A. Radkovskaya, M. Shamonin, T. Hao, C. J. Stevens, G. Faulkner, D. J. Edwards, and E. Shamonina, *physica status solidi (b)* **244**, 1170 (2007).
 - ¹⁸ J. Garcia-Garcia, F. Martin, J. D. Baena, R. Marques, and L. Jelinek, *J. Appl. Phys.* **98**, 033103 (2005).
 - ¹⁹ O. Sydoruk, A. Radkovskaya, O. Zhuromskyy, E. Shamonina, M. Shamonin, C. J. Stevens, G. Faulkner, D. J. Edwards, and L. Solymar, *Phys. Rev. B* **73**, 224406 (2006).
 - ²⁰ P. Gay-Balmaz and O. J. F. Martin, *J. Appl. Phys.* **92**, 2929 (2002).
 - ²¹ N. Liu, H. Liu, S. Zhu, and H. Giessen, *Nat Photon* **3**, 157 (2009).
 - ²² T. Q. Li, H. Liu, T. Li, S. M. Wang, J. X. Cao, Z. H. Zhu, Z. G. Dong, S. N. Zhu, and X. Zhang, *Phys. Rev. B* **80**, 115113 (2009).
 - ²³ B. Kanté, A. de Lustrac, and J.-M. Lourtioz, *Photonics and Nanostructures - Fundamentals and Applications* **In Press, Corrected Proof**, (2009).
 - ²⁴ J. Zhou, T. Koschny, M. Kafesaki, and C. M. Soukoulis, *Phys. Rev. B* **80**, 035109 (2009).
 - ²⁵ M. Decker, S. Linden, and M. Wegener, *Opt. Lett.* **34**, 1579 (2009).
 - ²⁶ R. Singh, C. Rockstuhl, F. Lederer, and W. Zhang, *Phys. Rev. B* **79**, 085111 (2009).
 - ²⁷ L. D. Landau and E. M. Lifschitz, *Electrodynamics of Continuous Media* (Pergamon Press, Oxford, 1984).
 - ²⁸ R. Marqués, F. Martín, and M. Sorolla, *Metamaterials with negative parameters* (Wiley, 2008).
 - ²⁹ R. Marqués, F. Mesa, J. Martel, and F. Medina, *IEEE Trans. Anten. Propag.* **51**, 2572 (2003).
 - ³⁰ M. Shamonin, E. Shamonina, V. Kalinin, and L. Solymar, *Microw. Opt. Techn. Lett.* **44**, 133 (2005).
 - ³¹ H. Liu, D. A. Genov, D. M. Wu, Y. M. Liu, J. M. Steele, C. Sun, S. N. Zhu, and X. Zhang, *Phys. Rev. Lett.* **97**, 243902 (2006).
 - ³² Computer Simulation Technology, <http://www.cst.com>.
 - ³³ The singularity of these integrals at $x = x'$ has been avoided by eliminating self-interaction between discrete current elements from the sum. We checked the correctness of this simplification by greatly increasing the meshing density, which did not result in any visible change in the interaction energy curves.